The British Journal of Radiology, 84 (2011), S338–S354

Imaging of thoracic aortic disease

[1]B J HOLLOWAY, MBChB, [2]D ROSEWARNE, FRCR and [1]R G JONES, MRCP, FRCR

[1]University Hospital Birmingham NHS Foundation Trust, Edgbaston, Birmingham, UK, and [2]New Cross Hospital, Wolverhampton, UK

ABSTRACT. Aortic pathology can be more complex to understand on imaging than is initially appreciated. There are a number of imaging modalities that provide excellent assessment of aortic pathology and enable the accurate monitoring of disease. This review discusses the imaging of the most common disease processes that affect the aorta in adults, with the primary focus being on CT and MRI.

DOI: 10.1259/bjr/30655825

Aortic pathology is often more challenging to understand and correctly diagnose with imaging than is initially appreciated. Aortic disease is often associated with significant morbidity and mortality. The clinical presentation is frequently non-specific and the pathology can often be discovered incidentally on imaging. The purpose of this article is to outline the common disease processes that affect the thoracic aorta in adults. The strengths and limitations of the differing imaging modalities are discussed, with an emphasis on CT and MRI. The pertinent imaging findings that have a noteworthy effect on management are illustrated. As open surgery is an established form of treatment, this review includes demonstration of the post-operative imaging findings, including potential pitfalls to interpretation. The newer endovascular treatments that are increasingly being used to treat aortic diseases are explored.

Imaging techniques

The imaging options available for assessment of the thoracic aorta include plain radiography, transthoracic echocardiography (TTE), transoesophageal echocardiography (TOE), multidetector CT, MRI and invasive catheter angiography.

The chest radiograph (CXR) can serve to raise suspicion of aortic disease by demonstrating an abnormal mediastinal contour in patients being investigated for other reasons. It can also indicate alternative pathologies when acute aortic pathology is suspected. However, it has been shown that radiographs alone are not sensitive enough to exclude aortic pathology or blunt aortic injury when it is clinically suspected [1, 2].

Echocardiography

Although TTE findings sometimes lead to a suspicion of aortic pathology that requires further evaluation, its limited windows and coverage mean that it cannot be regarded as a comprehensive technique for the evaluation of the aorta. TOE has high accuracy in assessing the aortic root, for example in proximal aortic dissection [3]. The benefits of TOE include the ability to obtain real time imaging in high resolution and to concurrently assess the aortic valve. However, it is an invasive procedure that is not straightforward to perform so is often reserved as a problem-solving tool when both the aortic root and valve are the prime source of interest.

Address correspondence to: Dr Benjamin Holloway, Queen Elizabeth Hospital, University Hospital Birmingham NHS Foundation Trust, Metchley Lane, Edgbaston, Birmingham B15 2TH, UK. E-mail: ben.holloway@uhb.nhs.uk

Computed tomography

In recent years, the speed, convenience, 24 h availability and excellent isotropic spatial resolution of multidetector CT (particularly for 16 slice machines and upwards) have led to this technique becoming pre-eminent in the evaluation of the acute aorta.

The precise technique and scan parameters are to some degree dependent on the specific CT machine. In the acute non-traumatic scenario, the evaluation of the aorta should start with a non-contrast-enhanced scan to detect acute aortic wall haematoma at least covering the arch to the diaphragm. A relatively thick 5 mm slice can be more useful than thinner sections as the resultant decrease in image noise and increased contrast enables the appreciation of the high-density rim of an acute intramural haematoma (IMH). In cases of follow-up in the non-acute situation, there is little indication for unenhanced components of the scan. This is then followed by a contrast-enhanced CT angiogram (CTA) reconstructed in thin slices of around 1 mm. A smooth algorithm CT reconstruction kernel is appropriate with the window settings ideally widened (such as level 200, width 800) to allow appreciation of abnormal filling defects with the bright contrast-filled aorta. Coverage should include the proximal great vessels from the arch and continue to the common femoral arteries (to allow planning of endovascular approaches and evaluation of visceral perfusion and complications). It is reasonable, however, to terminate scanning within the abdomen when it is clear the study is normal, which can result in a significant dose saving. Typically, infusion rates of 3–5 $ml\,s^{-1}$ of intravenous (iv) contrast containing 300–360 $mg\,ml^{-1}$ are used, preferably from the right arm to minimise artefact from dense contrast in the innominate veins. In most cases, triggering the scan by automated bolus tracking on the

aortic lumen will yield reliable aortic enhancement. Occasionally bolus tracking can provide suboptimal contrast, for example when the region of interest is incorrectly placed owing to anomalies or perhaps inadvertently placed in the false lumen of a dissection. Furthermore, aortic valve incompetence can lead to unpredictable contrast flow patterns, which can lead to erroneous early triggering if the region of interest is in the ascending aorta. For this reason, it is important that an experienced radiographer carefully observes the bolus tracking images and manually overrides the automated software when appropriate.

The main disadvantage of CT is the radiation dose, which is a particular concern in the young who require repeated imaging, as has been highlighted in recent mainstream medical literature [4]. Dramatic reduction in cardiac CT doses have been observed in recent times, partly related to low tube voltage techniques [5]. It is intuitive that such regimens could be applied to CTA with corresponding dose savings, but as yet there is little literature to confirm that comparable diagnostic accuracy will be achieved. The administration of iodinated contrast media may induce nephropathy, especially in those with pre-existing renal impairment, but the impact of a single bolus is questionable when weighed against not gaining the valuable information a CTA can provide [6].

Cardiac pulsation artefact mainly affects the aortic root in non-gated CTA and is more frequently present at slower heart rates [7]. The advent of electrocardiogram (ECG)-gated CT has made it feasible to acquire diastolic images of the aorta free from degradation by cardiac motion. For most scanners, β-blockade is usually required to obtain the slow, regular heart rates which are prerequisites for good quality imaging. In the acutely ill subject, when imaging can often be obtained out of normal working hours under the care of non-specialist radiologists and radiographers, this can be difficult to achieve. The penalty of using ECG gating is an increase in radiation dose, especially if retrospective gating is used. Although it is clearly advantageous to have gated images, there is little evidence that ECG gating should be regarded as essential for aortic imaging [8].

Magnetic resonance imaging

MRI mainly provides a useful adjunct to CT imaging of the aorta generally outside the acute setting. The lack of ionising radiation makes it particularly useful for the surveillance of younger patients with aortic pathology. A particular limitation of MRI is when there are metallic devices related to the aorta, such as stents, adjacent embolisation coils or occlusion devices, which often cause artefacts that preclude adequate evaluation. There are a number of sequences that are particularly useful for aortic imaging, all of which can be obtained in any prescribed plane.

''Black blood'' double inversion recovery spin echo

This sequence can be combined with ECG and respiratory gating to provide motion-free images of the aorta, and is particularly useful for assessing the wall of the vessel and for detecting slow flow or static blood within the lumen, *e.g.* in a dissection. A view of the chest can be obtained in a few seconds with a breath-hold technique and also gives a view of the surrounding lung, pleural spaces and chest wall.

Balanced steady-state free precession

This relatively new sequence is the mainstay of cardiac MRI but is also central to assessment of the aorta. These so called ''white blood'' cine sequences of the aorta can allow appreciation of flow disturbance within the lumen related to a stenosis. This subsequently allows planning of phase contrast sequences to determine peak velocity and degrees of regurgitation.

Phase contrast sequences

These use the changes in phase in flowing blood to calculate the direction of flow and velocity. They are most useful for assessing the peak velocity at sites of stenosis in the aorta (such as in coarctation), which can be used to estimate a gradient.

Non-contrast MR angiography sequences

These are the subject of renewed interest and use partly related to the concerns regarding a possible link between gadolinium and nephrogenic systemic sclerosis. One such example is balanced steady-state free precession (bSSFP) angiography, which enables a three-dimensional (3D) data set to be produced including motion-free images of the aorta when combined with ECG gating and respiratory navigation [9]. Depending on the regularity of the patient's breathing, ECG rhythm and the prescribed tolerance windows for image capturing, the volume data sets of the whole thoracic aorta can be obtained in only a few minutes. The disadvantage of this sequence is in the context of flow disturbance and high velocity when there can be failure to homogenise the blood pool, resulting in artefacts.

Contrast-enhanced MR angiography

This is well established as a means of assessing the aorta and produces consistently good quality 3D data sets. Using gadolinium as the contrast agent reduces the artefact from inhomogeneous flow as seen in non-contrast MR angiography (MRA) techniques. Standard techniques include injection of iv gadolinium at flow rates of 3–5 $m\,s^{-1}$ with timing determined by bolus tracking. Newer time-resolved fast MRA techniques enable multiple 3D data sets to be produced over a matter of seconds, which can aid the understanding of collateral flow [10]. Disadvantages are that only the lumen is demonstrated, and it obviously involves the iv administration of gadolinium.

There are a number of other sequences that can be used in specific situations. Ultra-fast gradient echo cine sequences were once the main sequence used in cardiac MRI but have been surpassed by bSSFP. However, when evaluating the aorta, which contains areas of disturbed high-velocity flow, these gradient echo cine sequences can be helpful as they tend to be less prone to flow-related artefacts than bSSFP. The high signal on T_1 weighted images associated with the methaemoglobin in subacute haematoma may provide useful extra information as to the age of an IMH. T_2 weighted images demonstrate oedema as high signal and can provide

useful information regarding the activity of inflammatory aortic conditions.

Invasive catheter aortography

This was once the gold standard in the evaluation of the aorta but has been rather superseded by CTA. Aortograms are now generally reserved for situations where a therapeutic intervention is planned or likely as part of the procedure. When choosing a modality, consideration should be given to the clinical scenario, radiation exposure, contrast issues and local expertise.

The normal aorta and common variants

The ascending thoracic aorta arises from the aortic valve annulus to the right of the midline and arches in a parasagittal plane to the left of the trachea to descend in the left paravertebral region, exiting the thorax via the diaphragmatic hiatus (Figure 1a). The aortic sinus is a focal annular bulge in the aortic contour which arises distal to the aortic annulus and connects to the tubular ascending aorta at the sinotubular junction. The left and right coronary arteries arise from the sinus above the left and right aortic valve cusps, with the posterior cusp normally having no associated artery. From the aortic arch arise the roots of the great vessels, most commonly comprising the innominate (brachiocephalic) artery, the left common carotid artery and the left subclavian artery. The transition between the arch and the descending aorta is called the isthmus and occurs at the ligamentum arteriosum, with the descending aorta extending to the diaphragmatic hiatus. The aortic wall is made up of three layers: a thin inner intima, a central elastic media and an outer fibrous adventitia (Figure 1b).

The aortic calibre varies in relation to age, gender and body surface area, so absolute figures are not valid for determining abnormality. Nevertheless, diameters in excess of 4.1 cm and 3 cm for the ascending and descending aorta respectively are invariably abnormal [11].

There are a number of common variants of the aorta and its branches that are comprehensively covered in other texts [12]. The commonest of these is the aberrant right subclavian artery arising distal to the left subclavian artery, coursing to the right and passing behind the oesophagus. This is only rarely associated with other anomalies and is usually of little significance. A right-sided aortic arch (aortic arch passing to the right of the trachea) is associated with two principal branching patterns: mirror image branching, which is associated with a high rate of congenital cardiac anomaly, and right aortic arch with aberrant left subclavian artery, which has a low association with other abnormalities.

Aortic aneurysmal disease

Thoracic aortic aneurysmal disease usually occurs as a result of degeneration of the media, but is also associated with the inherited conditions Marfan's, Loeys–Dietz, Ehlers–Danlos and Turner's syndromes. Aneurysms are often incidentally discovered on imaging, with the ascending aorta most commonly involved [13]. Absolute measurements are not a good predictor of the severity of abnormality, and measurements should be considered relative to age, gender and body surface area [14]. When aneurysms reach 6 cm in the ascending and 7 cm in the descending aorta, there is a distinct increase in the risk of

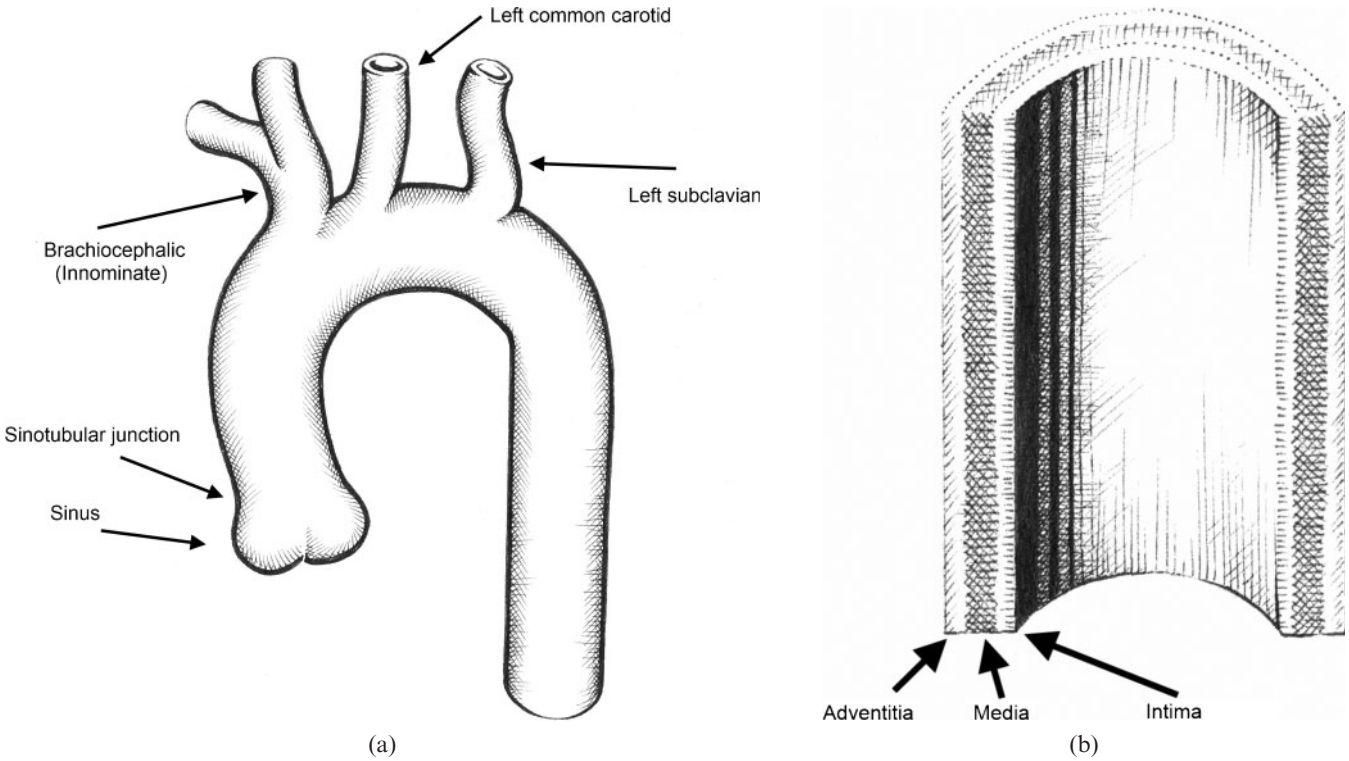

Figure 1. Diagrams depicting (a) the aorta and major branches, and (b) the layers of the aortic wall (courtesy of Dr Angela Luck).

rupture, dissection or death to around 14% per year, and treatment is therefore recommended at 5.5 cm and 6.5 cm diameter respectively [15]. When aortic aneurysms are found incidentally, it is advisable to seek a cardiothoracic opinion when the ascending and descending aortas are more than 4.5 and 5.5 cm, respectively, in diameter so that appropriate monitoring can be instituted. Normal growth rate of all types of thoracic aneurysms averages 0.12 cm per year [16]. More rapid growth than this (particularly if greater than 0.5–1 cm per year) and/or the development of symptoms, such as pain, should prompt urgent treatment [15].

The most common of the inherited conditions which cause aortic aneurysms is Marfan's syndrome, in which patients have a defect in the collagen making up the elastic media of the aortic wall. Most patients with this

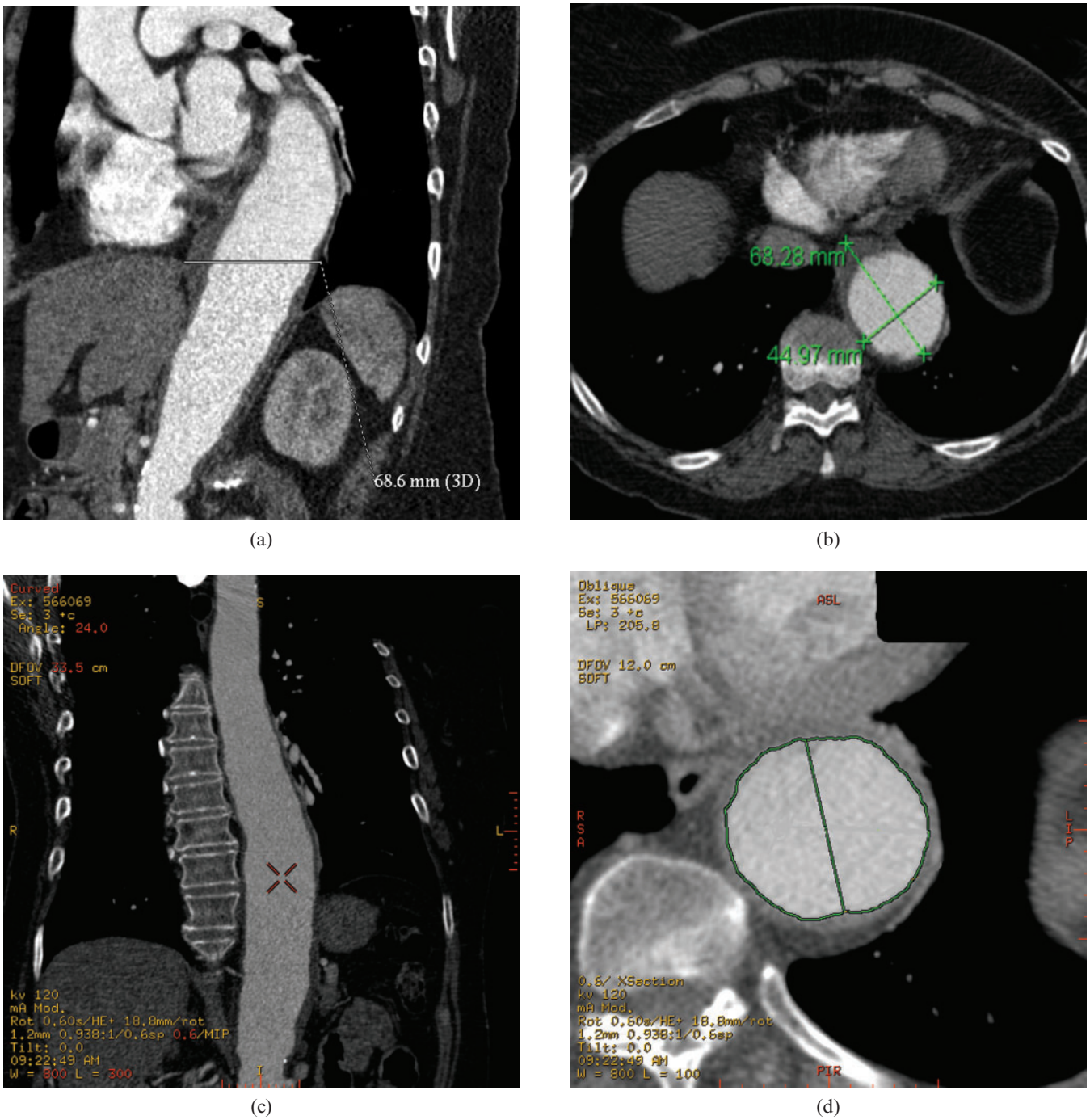

(a) (b) (c) (d)

Figure 2. Measuring perpendicular to the lumen is important in accurately determining the size of aortic dilatation. (a) CT angiogram (CTA) coronal multiplanar reconstruction (MPR) showing an inaccurate measurement oblique to the lumen in a tortuous aorta (~6.9 cm). (b) True axial CTA image shows this erroneous oblique measurement. The second short axis (~4.5 cm) measurement is more accurate. (c, d) Reconstructed curved MPR of the same CTA generates an MPR perpendicular to the centre line of the vessel. This gives the most accurate measurement but is considerably more time-consuming to generate. The true diameter is 4.5 cm. 3D, three dimensional.

disease develop aortic dilatation, particularly of the sinus, with characteristic effacement of the sinotubular junction. They demonstrate a greater tendency to dissection and rupture so intervention is recommended at smaller sizes [17].

Saccular aneurysms are less predictable and the dimensions given earlier are not applicable. Compared with degenerative fusiform aneurysms, there is a distinct lack of evidence on the precursors of rupture. Evidence of changing size or morphology is often used as a guide for the timing of intervention, but again there are no conclusive data to support this practice. Saccular aneurysms are often pseudo-aneurysms, in that their wall does not consist of all the normal aortic wall layers, and are described in relation to trauma, infection or penetrating atherosclerotic ulcers. These types of aneurysms, in the context of their aetiology, are discussed further below. Rupture of aortic aneurysms is usually fatal. Contained rupture, however, in the fortunate few, is well described and obviously requires immediate surgical referral.

The evaluation of thoracic aneurysmal disease is straightforward with CTA as the data set can be manipulated easily in multiple planes, allowing better appreciation of the anatomy and relationship of adjacent structures. CTA has good inter- and intra-observer agreement, making it ideal for monitoring aneurysms [18]. It is important to measure the diameter perpendicular to the vessel lumen. Hence, in a true axial CT slice the shorter diameter of the lumen is more representative of true vessel diameter (Figure 2). The latest software allows the reconstructions of curved multiplanar reconstructions (MPRs) with automatic true perpendicular measurements of the lumen, but this can be quite time-consuming. Indeed, while MPR and 3D reconstructions can aid in surgical planning, they have not been categorically shown to improve diagnostic accuracy [19] (Figure 2). On CTA, acute rupture of aneurysms is seen as extensive ill-defined heterogeneous peri-aortic soft-tissue haematoma, sometimes with a focal new saccular pseudo-aneurysm or contrast blush of active extravasation at the site of rupture (Figure 3). Pleural effusions or haemothoraces are also often seen.

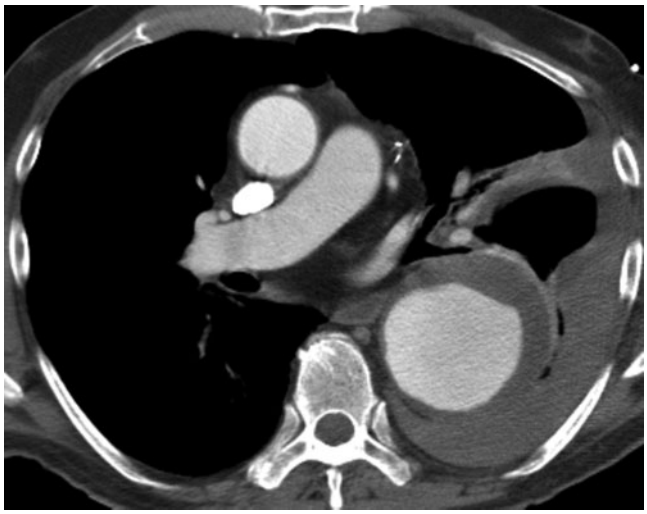

Figure 3. Ruptured descending aortic aneurysm. The CT angiogram demonstrates the peri-aortic haematoma and left haemothorax characteristic of rupture in this man who presented with acute chest pain. The peri-aortic tissues contained the leak long enough for him to undergo successful endovascular stenting.

Compared with CT, there is relatively limited corroborative evidence of the accuracy of MRI in assessing aortic aneurysms. When diagnosing all types of thoracic aortic disease, including aneurysms, contrast-enhanced MRA (CE-MRA) performed well compared with surgery and other forms of imaging [20]. Clearly MRI is a preferable alternative for younger patients to eliminate radiation issues, and when performed without gadolinium is useful in those with renal impairment. The newer non-contrast-enhanced bSSFP MRA sequences have similar accuracy to CE-MRA [21]. As these sequences are quick and simple to perform, they have the potential to play a major role in the efficient follow-up of aneurysms in the future.

Acute aortic syndromes

Acute aortic syndromes carry high mortality and morbidity and early recognition of these conditions is vital to ensure prompt treatment [22]. Dissection, IMH, penetrating atherosclerotic ulcers (PAUs), and traumatic partial or total rupture are the primary pathologies in this group. They can share common imaging features, occur together or be directly related.

Aortic dissection

Sometimes called classic aortic dissection, this is the most common acute aortic condition. It consists of an intimal tear which allows blood to penetrate the aortic wall media forming a false lumen with re-entry at a variable distance further down the vessel. Hypertension is

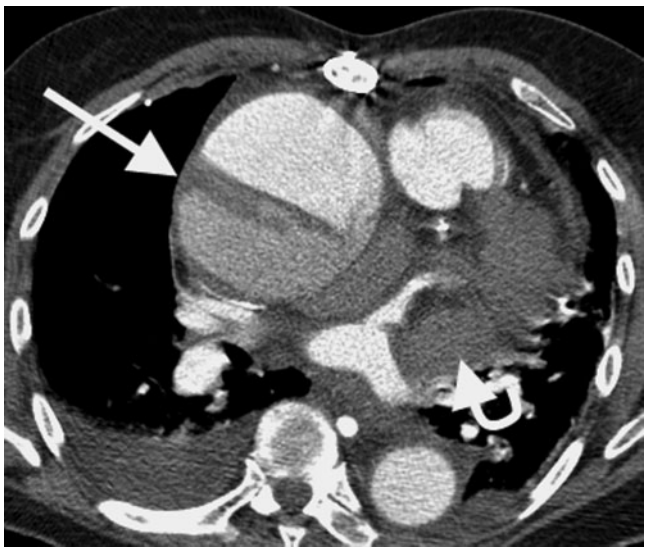

Figure 4. Acute Type A ascending aortic dissection in an already aneurysmal aorta. The false lumen has partial thrombosis (the straight arrow) and there is a haemopericardium which compresses the left atrial appendage (curved arrow). This carries a high mortality because of the potential for cardiac tamponade and requires emergency surgical treatment.

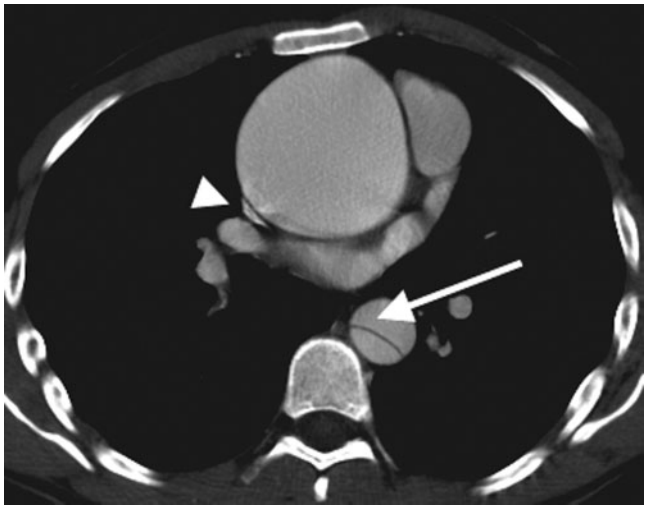

Figure 5. This 24-year-old man with Marfan's syndrome presented with acute chest pain. He has a large ascending aortic aneurysm but the separate Type B dissection in the descending aorta was the cause of the acute presentation. The arrow demonstrates the acute angle between the intimal flap and the aorta wall, indicating that the false lumen is anterior, which is important to determine if endovascular treatment is contemplated. The superior vena cava is compressed by the ascending aortic aneurysm (arrowhead).

the most common predisposing factor. In younger patients Marfan's syndrome is common, and an initial CTA or MRI may reveal other associated findings such as dural ectasia and pectus deformity [23, 24]. The Stanford classification is widely accepted and guides the need for surgery by dividing dissection into Type A, commencing proximal to the left subclavian artery, and Type B, commencing distal to this point. Type A dissection carries a high risk of early mortality, most commonly from cardiac tamponade and myocardial infarction (secondary to extension into coronary arteries), and so is treated with surgery [25] (Figure 4). Type B dissection is treated medically (primarily with control of hypertension) and requires long-term follow-up with imaging to identify aneurysmal dilatation, which is more frequently seen when flow persists in the false lumen [26].

There remains controversy when a Type B descending aortic dissection extends proximally only into the arch as to the type and need for surgery [13]. A systematic review comparing the accuracy of TOE, CTA and MRI for the acute diagnosis of dissection found little difference between the techniques [3]. The ready availability of CTA and the widespread radiological familiarity with the technique within departments make it the modality of choice [22]. On CT, the identification of a linear filling defect within the lumen representing the intimal flap is the characteristic feature. The false lumen is most reliably identified by the acute angulation between the flap and the wall (beak sign) and its larger cross-sectional area [27] (Figure 5). It is important to identify the false lumen and site of intimal tear if an endovascular procedure is planned. It is, however, equally important to detect end-organ malperfusion, for example when the intimal flap extends into the renal artery or intermittently drapes over its ostium, resulting in ischaemia or infarction of the kidney manifesting as poor enhancement on CTA. This may be prevented or limited with timely radiological stent placement [28].

There are pitfalls when interpreting CT for dissection. The most important of these is cardiac motion at the aortic root, which results in linear filling defects occurring anteriorly and posteriorly which do not continuously extend into the ascending aorta. This is usually straightforward to recognise, but if there is doubt it can be eliminated by ECG-gated CT [29]. Less

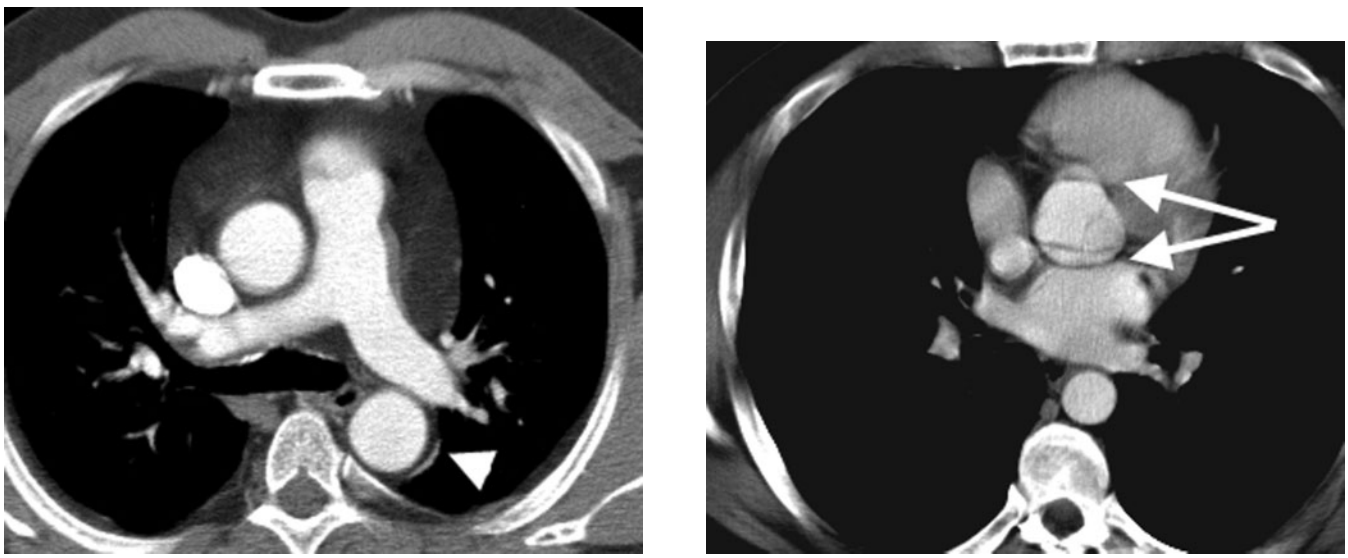

(a) (b)

Figure 6. Pitfalls that mimic aortic dissection. (a) Lung atelectasis adjacent to the thoracic aorta (arrowhead) which can be appreciated as not being dissection as it lies outside the aortic adventitia. (b) Cardiac-related motion of the aortic root at the level of the aortic sinus (arrows). This is usually straightforward to appreciate as it typically occurs anteriorly and posteriorly and does not continuously extend into the ascending aorta without interruption.

Figure 7. This patient, who has several comorbidities, presented with chest pain. Only a post-contrast study was performed, which shows a focal out-pouch of contrast into the atheroma in the distal arch typical of a penetrating atherosclerotic ulcer. Some of the aortic wall thickening resolved on subsequent follow-up CT angiogram making it likely to have been an intramural haematoma (IMH). A non-contrast-enhanced CT would have helped by showing the acute IMH as a hyperdense rim.

commonly, lung atelectasis can drape over the descending aorta, and streaks in the ascending aorta from high-density contrast in the superior vena cava can be mimics (Figure 6).

Penetrating atherosclerotic ulcers

PAUs were first described in 1986 by Stanson et al [30]. These are defined as an atherosclerotic lesion that penetrates the elastic lamina, usually leading to a haematoma within the media, but also potentially to true dissection or rupture. This lesion is primarily a diagnosis made on imaging, with even the larger series having limited pathological correlation. As PAUs can cause IMH and classic dissection, the correct diagnosis of this lesion is not always easy to make on imaging [31]. On CT they appear as focal protrusions of contrast through atheroma into the aortic wall (Figure 7), invariably in a patient with significant generalised atherosclerotic disease. They most commonly occur in the descending aorta [32] and can lead to an acute presentation, usually with pain. Irregular atheroma containing non-penetrating ulcers or chronic intraluminal thrombus can be indistinguishable from PAUs on CTA. It is for this reason that a non-contrast-enhanced CTA is vital in all cases of suspected acute aortic syndrome as this enables the associated hyperdense acute IMH to be differentiated from chronic irregular atheroma or intraluminal thrombus. In cases when a non-contrast-enhanced CT has not been performed and there are equivocal appearances on CTA, MRI can aid in the diagnosis of PAUs by identifying the acute IMH [33].

Intramural haematoma

Spontaneous acute IMH can be observed without any imaging features of intimal flap or penetrating atherosclerotic ulcer. This phenomenon was first described by Kruckenberg in 1920 and is best described as ''intramural haematoma without intimal flap'' [34]. Some postulate spontaneous IMH as secondary to rupture of the vasa vasorum, the capillary network in the aortic adventitia and media [35]. However, there is little pathological proof of this and it remains possible they are secondary to imperceptible microscopic intimal tears (therefore are effectively a type of limited dissection in which the false lumen is completely thrombosed).

As with dissection, IMH is associated with hypertension but tends to be seen more in older patients and disproportionately in the descending aorta [36]. A classic double-barrelled dissection in which the lumen is completely thrombosed at the time of initial imaging is indistinguishable from an IMH, which is why these conditions are described as having considerable overlap in natural history and require similar treatment [37].

Acute IMH appears as a crescentic hyperdense rim in the aortic wall on non-contrast-enhanced CT, which is the most useful identifying feature. The CTA enables

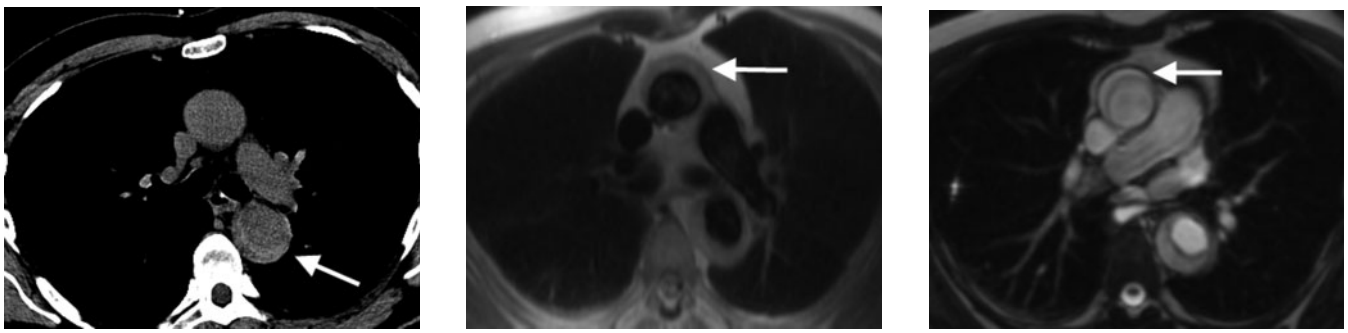

(a) (b) (c)

Figure 8. A 66-year-old male presented with acute chest pain. He was allergic to iodinated contrast media so initially underwent a non-contrast-enhanced CT angiogram (a), which shows the hyperdense rim of an intramural haematoma (IMH) in the descending aorta (arrow). MRI was performed to determine if the ascending aorta was involved, which is confirmed (horizontal arrows) with ''black blood'' half-Fourier acquisition single-shot turbo spin echo (b) and balanced steady-state free precession images (c). IMH has a similar natural history to dissection so is often treated in a similar manner, and this man underwent successful surgery with grafting of the ascending aorta.

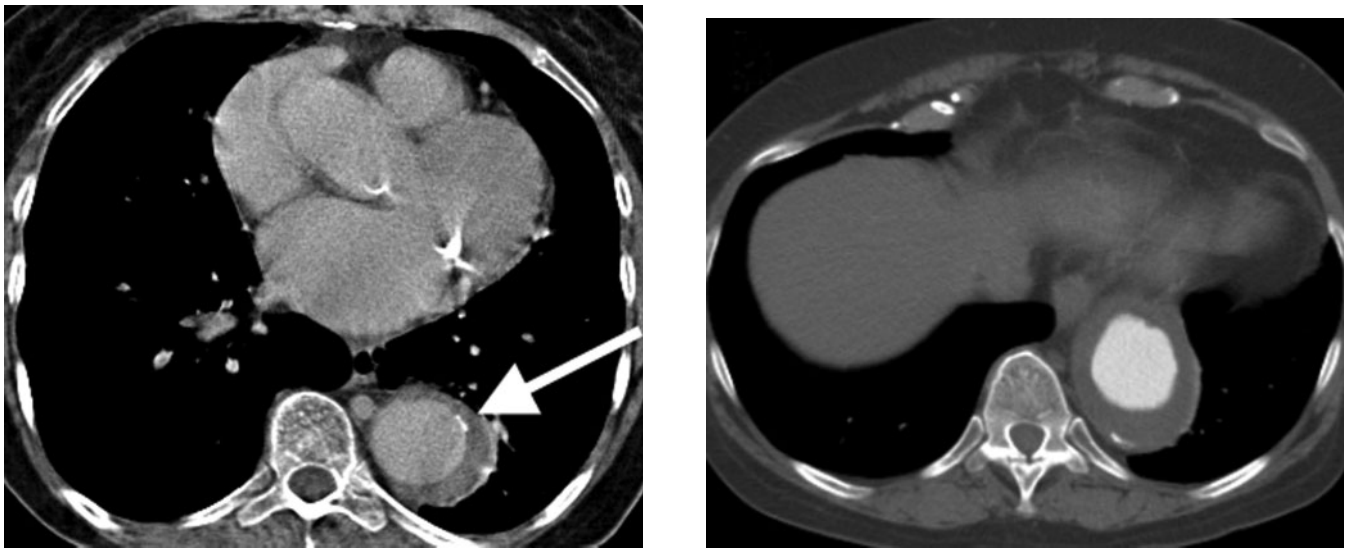

(a) (b)

Figure 9. Two CT angiograms on different patients demonstrating the difficulty differentiating extensive intramural haematoma (IMH) from intraluminal thrombus in the aorta. (a) A patient with an extensive IMH involving the descending aorta. The clue that this is not simply intraluminal thrombus is the displacement of intimal calcification (arrow). (b) A different patient in whom there is intraluminal thrombus accumulating in an ectatic section of the descending aorta. The intimal calcification is not displaced. Sometimes chronic intraluminal thrombus can develop calcification within it, which can make it more difficult to differentiate.

differentiation of IMH from dissection by demonstrating no contrast flowing in the false lumen (Figure 8). Calcified atheroma on the displaced internal intima can be a useful sign to differentiate an extensive IMH from chronic smooth intraluminal thrombus on CTA (Figure 9). Contrast can develop in the haematoma on follow-up imaging of IMH as new ''ulcer-like projections''. These can be related to a new intimal tear, penetrating ulcer or a branch pseudoaneurysm and can enlarge, reduce in size or be incorporated in general enlargement of the lumen [38]. It is uncertain if these are a marker for a poorer prognosis, although there is some evidence that those sited in the arch and proximal are more significant [39]. As in PAUs and secondary IMH, MRI can also demonstrate this condition well and serves as a good modality to clarify equivocal cases [40].

Acute aortic syndrome in blunt trauma

Thoracic aortic injury is one of the leading causes of death in major blunt trauma and involves the partial or

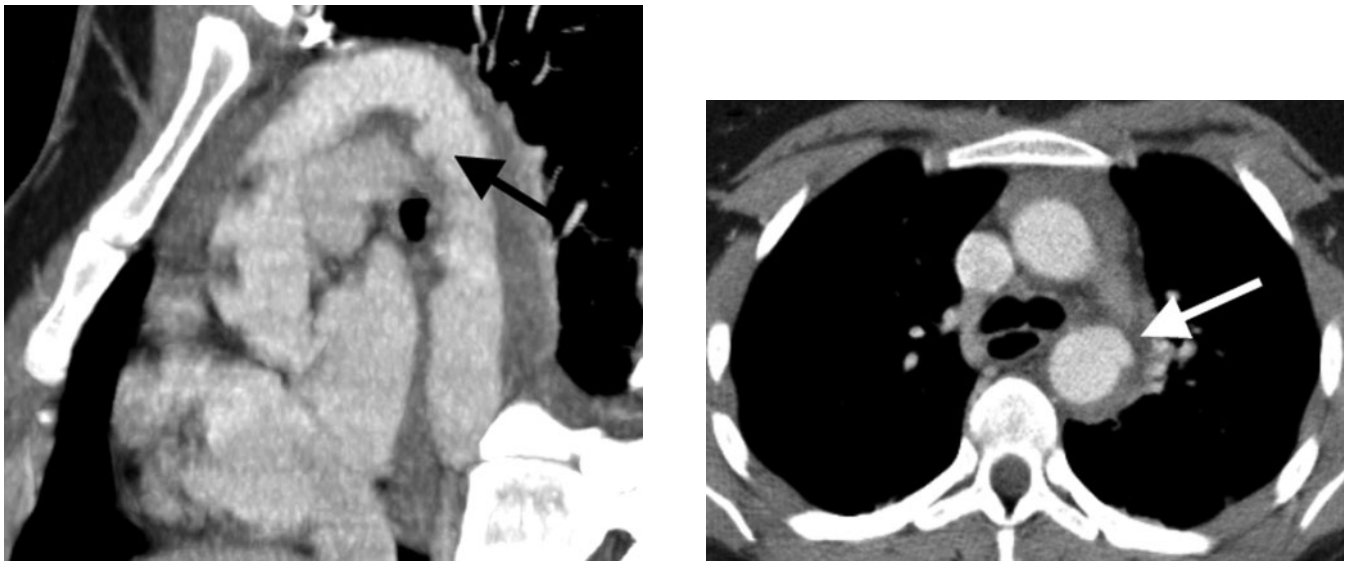

(a) (b)

Figure 10. CT angiogram (CTA) in a young female patient who was involved in a high speed road traffic accident. (a) Sagittal oblique multiplanar reformat of the CTA showing the subtle pseudo-aneurysm at the aortic isthmus (black arrow). (b) True axial image showing the subtle aneurysm (white arrow), which is only visible on a few slices. In major trauma, the direct signs of aortic injury can often be subtle and so it is imperative that the aorta is carefully assessed.

Figure 11. This man was found to have an incidental large saccular aneurysm arising from the proximal descending aorta. He had a history of significant trauma in the past so this was regarded as a chronic post-traumatic pseudo-aneurysm.

total transection of the aortic wall [41]. There are a number of theories as to the mechanism behind thoracic aortic injury [42]. Shearing or bending forces at the junction between fixed and mobile points of the aorta are thought to occur at the aortic isthmus. Torsion stress is also said to occur in the ascending aorta. Osseous pinching of the aorta between the sternum and the spine has been proposed more recently based on evidence from a simulated animal model and retrospective review of a small cohort of trauma victims [43, 44]. The aortic isthmus is the classic site for observing injury on imaging [41]. Injuries at other sites, particularly the ascending aorta, are also well recognised and are possibly under-represented in the imaging literature owing to a higher attrition rate at the scene [41].

CTA is used extensively in trauma and provides excellent views of the thoracic aorta. On CTA, the direct signs of aortic injury are dissection, IMH, pseudo-aneurysm, contour irregularities and intimal flaps (Figures 10 and 11). These are very accurate at detecting aortic injury and effectively render diagnostic invasive catheter angiography obsolete [45]. Indirect signs such as mediastinal haematoma are neither sensitive (blood can stay contained) nor specific (rupture of minor mediastinal vessels can also cause this) for aortic injury and should not be relied upon [46].

Aortic coarctation

Aortic coarctation is the most common congenital defect, making up around 7% of all congenital heart lesions [47]. It consists of a focal stenosis, commonly at the aortic isthmus (between the left subclavian artery and ligamentum arteriosum), but can occur in a more tubular fashion in the mid-aortic arch. It continues to be difficult to definitively treat despite the accumulation of extensive experience since the first corrective operation in 1945 [48]. The challenge for surgical treatment in neonates and young children is to repair the stenosis but enable some means for the patient to grow without the stenosis recurring. Open surgical techniques include end-to-end

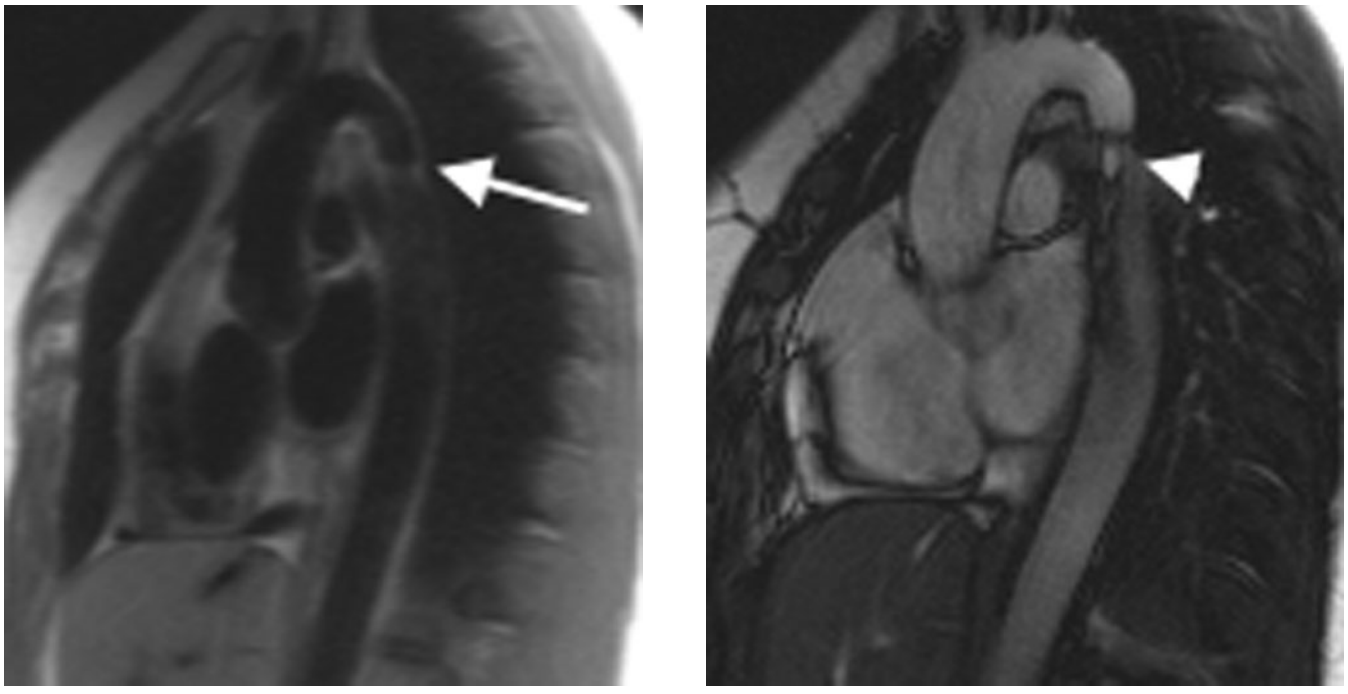

(a) (b)

Figure 12. Coarctation in a 19-year-old female with hypertension. (a) MRI ''black blood'' half-Fourier acquisition single-shot turbo spin echo sequence shows the anatomical narrowing (arrow). (b) Image from a cine balanced steady-state free precession sequence demonstrates the stenotic jet (arrowhead). Performing a phase contrast study perpendicular to this enables the peak velocity and subsequently the gradient across the stenosis to be estimated.

anastomosis, subclavian flap repair, synthetic patch repair, interposition grafting or bypass grafting. These techniques have led to long-term survival, but late complications are not unusual so these patients require monitoring with imaging [49, 50]. Resection of the stenosed segment and end-to-end anastomosis has a very good medium-term outcome but is not always technically possible if the affected segment is too long [51]. Subclavian flap repair involves dividing the subclavian artery a short distance from its origin and using the proximal-most artery to reconstruct the aorta at the site of coarctation. This provides acceptable long-term outcomes but can affect ipsilateral limb development [52]. Patients undergoing synthetic patch repair have a greater tendency to develop aneurysms than other repair types [53].

Although surgery is the primary treatment modality in children, endovascular treatment of coarctation with balloon angioplasty and stenting is used increasingly in adults [54]. This technique is showing encouraging short- and medium-term outcomes but has limited long-term data compared with surgery [55]. It is recognised that the continued monitoring of patients with stents is required to assess for complications such as aneurysm formation [56].

The ability of MRI to produce multiplanar images and assess velocity without radiation makes it the perfect modality for the follow-up of repaired coarctation in this young patient cohort who require repeated imaging. MRI has been proven to be more accurate and cost-effective for follow-up than echocardiography [57, 58]. A combination of ''black blood'' spin echo inversion recovery and bSSFP still images in axial and sagittal oblique planes usually demonstrate the anatomical narrowing (Figures 12 and 13). The newer bSSFP non-contrast-enhanced MRA sequences have the potential to increase accuracy of assessment while avoiding the need for gadolinium-enhanced MRA [21]. Gadolinium-enhanced MRA is the most well-established and validated sequence for assessing coarctation and is recommended, at least for the initial assessment [59]. This is particularly important when assessing small collateral vessels. bSSFP cine images in a prescribed sagittal oblique plane can demonstrate the flow disturbance associated with the coarctation. It is important that the phase contrast studies are correctly aligned perpendicular to a perceived dephasing ''jet'' distal to the stenosis so that the maximum velocity and an estimated gradient (using the modified Bernoulli equation) can be accurately determined [60] (Figure 12). A second phase contrast study in the distal aorta can also be helpful to assess for flow recruitment from collateral vessels draining into the descending aorta, which helps determine the severity of the stenosis [61]. At the same time, MRI allows the gold standard evaluation of left ventricular size, function and mass to be performed to assess the impact of the increased afterload on the heart.

MRI is technically possible and safe to perform in those who have undergone stenting, but is of limited value as signal drop-out artefact, particularly from steel stents, can obscure the images significantly [62]. MRI still has some value in that it can be successfully used to determine the extent of collateral flow which, as stated earlier, is a marker for the degree of stenosis [63]. Because of the limitations of MRI, CTA is the primary modality used for stent follow-up. (Figure 13). As already stated, CT is accurate in depicting aneurysms and dissection, which are recognised complications. Case reports also show that CTA can also detect stent fracture and secondary aortic rupture [64, 65].

Inflammatory and infective aortic disease

Takayasu's disease is a multisystem disorder that is characterised by a large vessel vasculitis resulting in wall thickening, stenoses, aneurysm formation and rupture of the aorta and its main branches [66]. It is generally, but not exclusively, seen in young adults, more commonly from Asia, and is associated with raised inflammatory markers [67] (Figure 14). Cross-sectional imaging has now surpassed invasive angiography as the recommended initial imaging modality owing to its ability to depict the wall of the aorta, not just the lumen [68]. CTA shows the thickened vessel wall and allows accurate assessment of

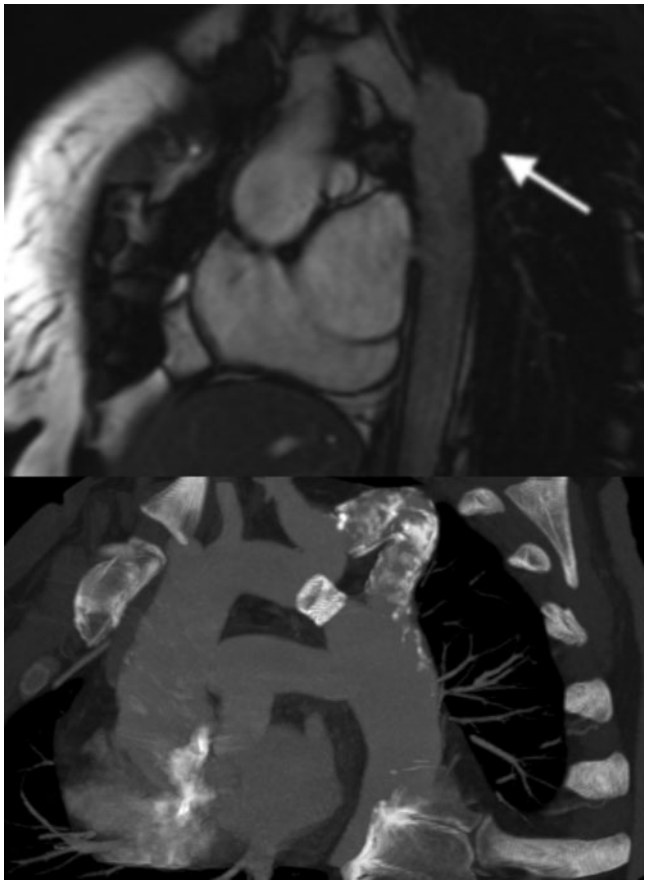

Figure 13. Coarctation repair complications. (Top figure) Sagittal oblique balanced steady-state free precession image demonstrating aneurysm formation in a 29-year-old woman, which is a common complication of synthetic patch repair (arrow). (Bottom figure) Sagittal oblique maximum intensity projection in a 41-year-old man with a recurrent coarctation which was initially treated with a bypass graft. The graft eventually became calcified and stenosed (after many years), so a stent was placed in the original native coarctation to relieve the obstruction.

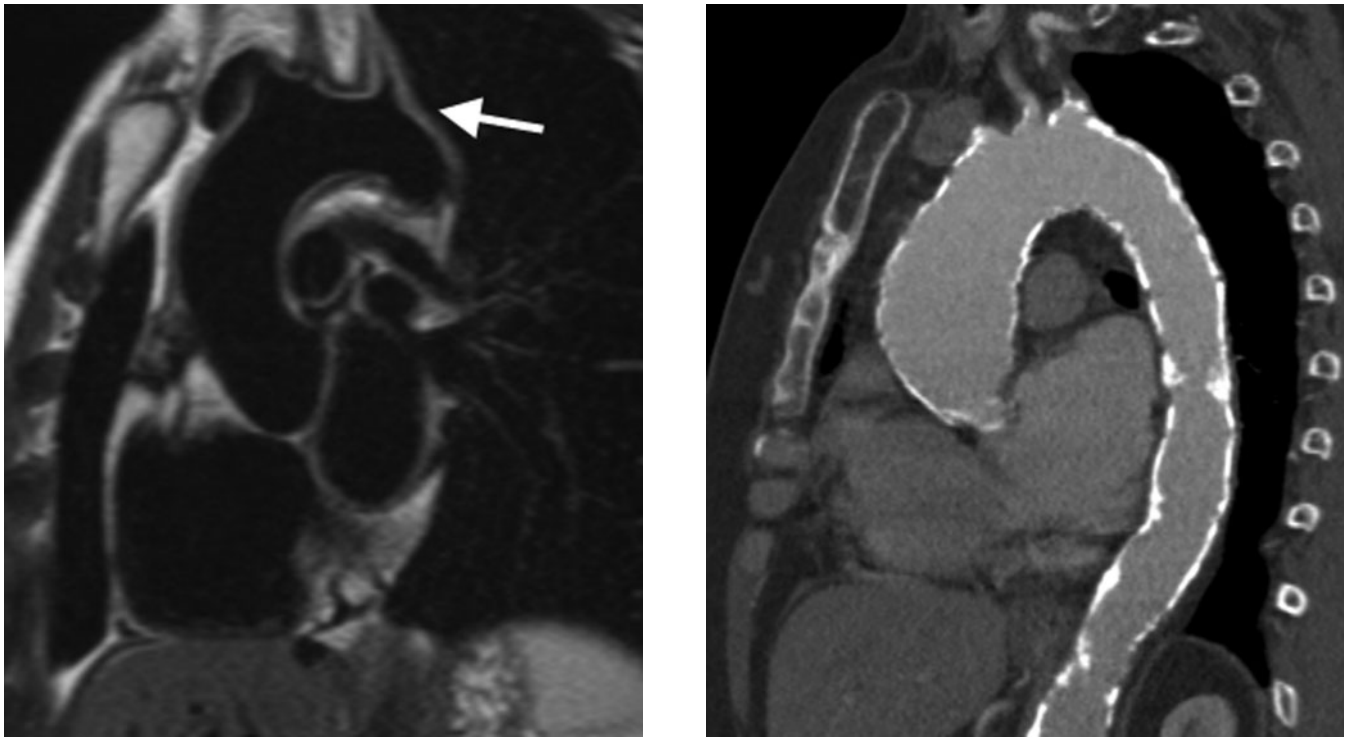

(a) (b)

Figure 14. Two patients with Takayasu's disease. (a) Sagittal oblique half-Fourier acquisition single-shot turbo spin echo ''black blood'' image which is the ideal sequence for demonstrating the diffuse thickening of the aortic wall and branches for the arch (arrow). (b) Contrast-enhanced CT angiogram sagittal oblique multiplanar reformat image of a patient with chronic disease with a diffusely calcified aorta.

aneurysm size, morphology and location, as well as documenting the degree of stenosis [69]. MRI can be particularly useful for assessing the acute and chronic phases of disease. The ''black blood'' double inversion spin echo (half-Fourier acquisition single-shot turbo spin echo, HASTE) sequence is particularly useful as it demonstrates the thickened vessel wall [70]. Contrast enhancement of the aortic wall disproportionate to the myocardium has been used as a marker of ongoing inflammation in the chronic phase [71]. The sensitivity of T_2 weighted MR images to oedema associated with inflammation makes it the ideal imaging modality to also help monitor the disease [72]. Other inflammatory conditions of the aorta are much rarer and include giant cell arteritis and Behçet's disease. These conditions affect the aorta much less frequently than Takayasu's disease, but are a recognised cause of aneurysm, dissection and rupture [73, 74].

Infection of the aorta often leads to aneurysm formation and results in high levels of morbidity and mortality [75]. The most commonly reported causative organisms are staphylococcus and streptococcus, but salmonella has also been implicated [76, 77]. As with other aneurysms, CTA is commonly used in the initial assessment. They are most frequently seen in descending and abdominal aorta, usually with a saccular morphology [78]. Differentiation from degenerative aneurysms is not always straightforward. However, on CTA, features including a surrounding inflammatory mass and fluid and less frequently disruption of the aortic wall calcification and periaortic gas should arouse suspicion [79] (Figure 15).

Imaging after surgically treated aortic disease

Thoracic aortic surgery is generally performed and followed up in the major tertiary centres. The long-term success of such surgery means there is a growing post-surgical population that will undergo imaging in non-specialist centres for other reasons. Open surgery involves the replacement of the diseased segment with a graft which is usually interposed but can be included with the diseased segment wrapped around the graft.

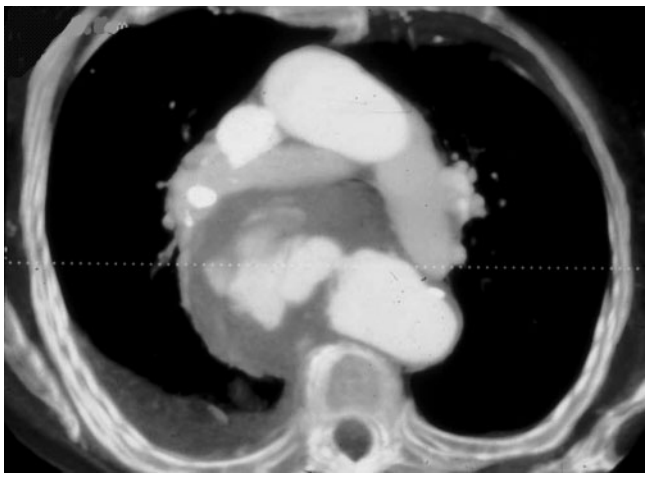

Figure 15. Rupture infected descending aortic aneurysm. This was successfully resected and the causative organism was found to be salmonella.

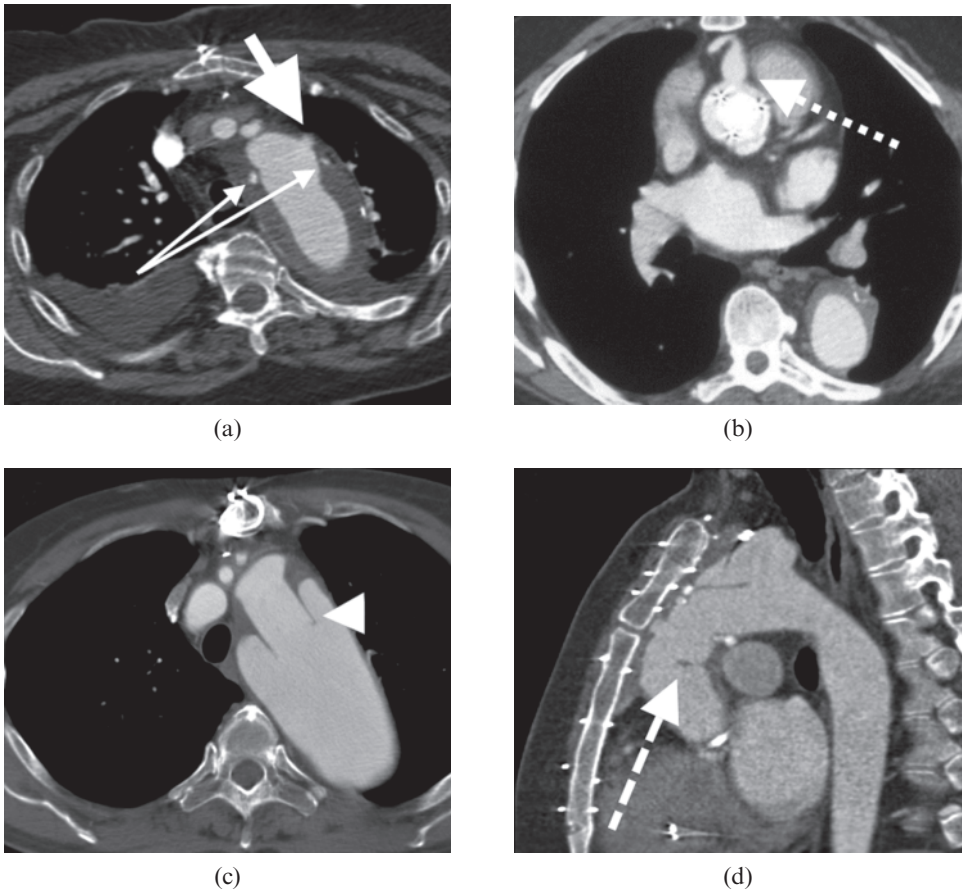

Figure 16. CT angiogram images showing normal findings in patients who have undergone either root, ascending aortic or arch replacements. (a) Typical contrast out-pouch of the reperfusion port (big arrow) and the high-density felt material that lines the anastomosis to reinforce it (narrow double arrow). (b) Typical appearance of a coronary button (dotted arrow), which consists of a circular section of native aorta: this was used to aid anastomosis of the coronary artery to the new interposition graft replacing the root. (c) Typical elephant trunk appearance whereby the interposition graft extends into the native proximal descending aorta (arrowhead). This can then be used to anastomose any subsequent grafts that are required to replace the descending aorta in the future. (d) Graft fold in the ascending aorta (dashed arrow). These are commonly seen and very rarely cause any significant haemodynamic effect or clinical issues. This patient also has residual dissection in the arch which was not replaced.

The mortality associated with surgery is generally low (in the order of 1–5%) but is significantly higher with the more complex thoraco-abdominal repairs and when there are significant comorbidities [13].

Grafts appear as a thin hyperdense rim on pre-contrast scans. After contrast, this rim is obscured but can usually be differentiated from native aorta by its uniform calibre, by being more circular in cross-section and having proximal and distal anastomotic sites. The anastomoses are recognised by a change in calibre and by higher density felt buttressing material which is applied to reinforce the anastomosis [80, 81]. There are a number of pitfalls to interpreting post-operative CT scans (Figure 16). The felt material could be misinterpreted as extravasated contrast or pseudo-aneurysm, but this is easily clarified with a pre-contrast CT showing it as high density. Common normal findings that can be easily be misinterpreted as pseudo-aneurysms are coronary buttons at the origin of the coronary arteries and bypass cannula sites (Figure 13). The graft can often have points of pronounced angulations or kinks which are rarely of haemodynamic significance but can be mistaken for an intimal flap. A commonly used two-stage approach is the elephant trunk, which involves initial replacement of the ascending aorta and arch with an interposition graft that is then allowed to extend into the lumen of the descending aorta (Figure 13). The purpose of this is to allow a second graft to join onto this should the already diseased descending aorta subsequently require replacement. To the unfamiliar, the elephant trunk can mimic the proximal portion of a Type B dissection, but the lack of continuation into the distal aorta and its tubular nature usually allow differentiation. It is normal to see perigraft low (near fluid) attenuation material without enhancement surrounding the graft in the early post-operative period. Indeed, this can often persist for as long as a year after surgery without adverse consequences and therefore this alone should not be regarded as evidence of a complication [81]. Persisting gas in the mediastinum beyond 6 weeks should raise the suspicion of infection or fistula formation to adjacent bronchus or oesophagus [80]. Complications of aortic surgery may only be detected incidentally on CT performed for other reasons and mainly include pseudo-aneurysms at the anastomoses and infection.

Endovascular treatment of aortic disease

Minimally invasive endovascular management for acute and chronic aortic pathology has emerged over the past two decades as an alternative to open surgery with the rapid development of the technology, understanding and supporting evidence [82–84].

Endovascular management is now indicated for most thoracic aortic pathologies [85, 86]. The longevity of endografts is controversial; however, recent assessment of short- and mid-term endografts demonstrates durability similar to, if not better than, open surgery but with the need for more secondary interventions [84]. In addition to aneurysmal disease, dissections and traumatic lesions are all recognised indications for endovascular management. Ascending and arch aortic pathology are usually not suitable for exclusive endovascular repair; however, hybrid procedures are possible in these circumstances.

Surgery is often favoured in younger patients. However, in acute trauma, endovascular management has a much lower mortality and complication rate and is the treatment of choice in this situation [87] (Figure 17).

More favourable outcomes are reported with endovascular repair than surgery if there is significant comorbidity. Periprocedural mortality rate is of the order of 6% with endovascular repair, and can be much higher with open surgery [84, 88, 89]. The mean incidence of periprocedural stroke is 2.7% and of paraplegia is 2.2% [90]. A long endograft and distal placement are associated with an increased risk of spinal cord ischaemia [91]. Coverage of the artery of Adamkiewicz, spinal branches of intercostal trunks or vertebral arteries are usually responsible for spinal cord ischaemia and should be considered as a potential complication when placing an endograft at the T1–T8 region.

Prior CTA and pre-deployment angiography are vital to assess the morphology of the aorta and spinal arteries [92]. At least 15 mm proximal and distal landing zones of adequate calibre vessel without occluding a branch are ideal. The left subclavian artery can be covered with varying outcomes ranging from a fourfold increase in stroke and paraplegia to no significant increase in complication rate if a more selective approach is adopted [90, 93]. Pre-procedural left subclavian bypass surgery can be carried out, especially if there is a hypoplastic right vertebral artery. There are a number of commercially available devices with a spectrum of clinical data supporting their use. These devices may differ in terms of their individual technical features, properties and sizes but essentially all are based on a self-expanding covered stent–graft principle. The metallic stent component provides the structural strength and the graft material the exclusion of surrounding pathology. All devices have radio-opaque markers delineating the extent of the graft portion, which varies according to manufacturer. Delivery systems are typically 22-French sheath, and external iliac arteries need to be at least 7–8 mm for safe delivery. If these requirements are not met, then surgical access manoeuvres can be considered.

Some examples of available devices include the Medtronic Valiant system (Medtronic, Santa Rosa, CA), which consists of a self-expanding nitinol stent covered with a polyester graft. This device is available in a straight and tapered design with diameters of 24–46 mm and lengths up to 227 mm available. Another example is the Gore TAG device (WL Gore, Flagstaff, AZ). This consists of a nitinol exoskeleton with a polytetrafluoroethylene lining. This device is available in diameters of 26–45 mm with 10, 15 or 20 cm lengths. The Cook Zenith TX2 system (Bloomington, IN) consists of a stainless steel self-expanding stent with a Dacron graft. This is available in diameters ranging from 22 to 42 mm and lengths of 10–22 cm. Initially, a conventional angiogram is carried out in a left anterior oblique projection prior to deployment to delineate branch vessels and the pathology. Lowering the blood pressure pharmacologically prior to device deployment can prevent displacement of the graft and facilitate more accurate positioning. Surveillance of endografts with annual CTA is essential to monitor for complications (Figure 18). Complications can be immediate and these are usually related to misplacement or migration of the endograft or related to the access site. Later

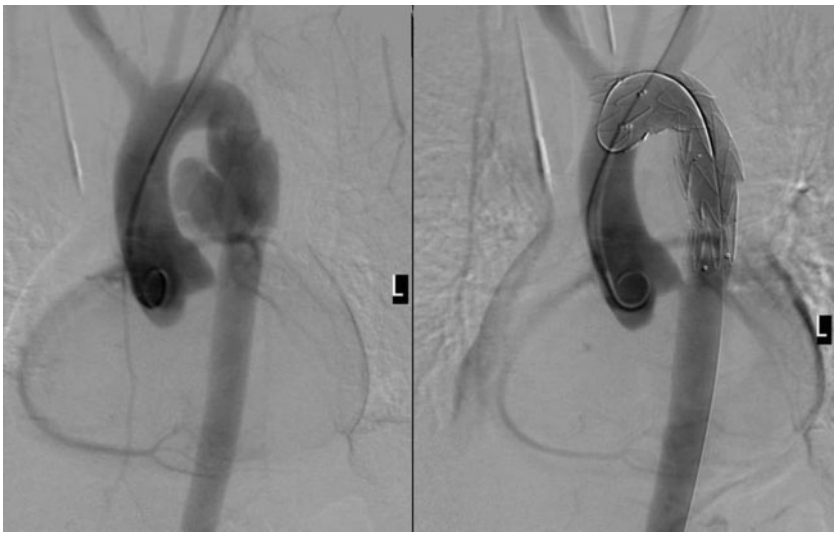

Figure 17. Stent-grafting of traumatic aortic rupture at level of isthmus. The image on the right is taken post endograft deployment demonstrating adequate repair. Laminar arterial flow was observed on gaining access to the femoral artery for endograft deployment. This corresponded to a lack of pulsation contractility due to massive aortic injury. On the post-deployment digital subtraction angiography, the left subclavian artery is covered by the covered portion of the endograft; however, the leading 12 mm of the device is uncovered and flow is maintained in the left common carotid artery.

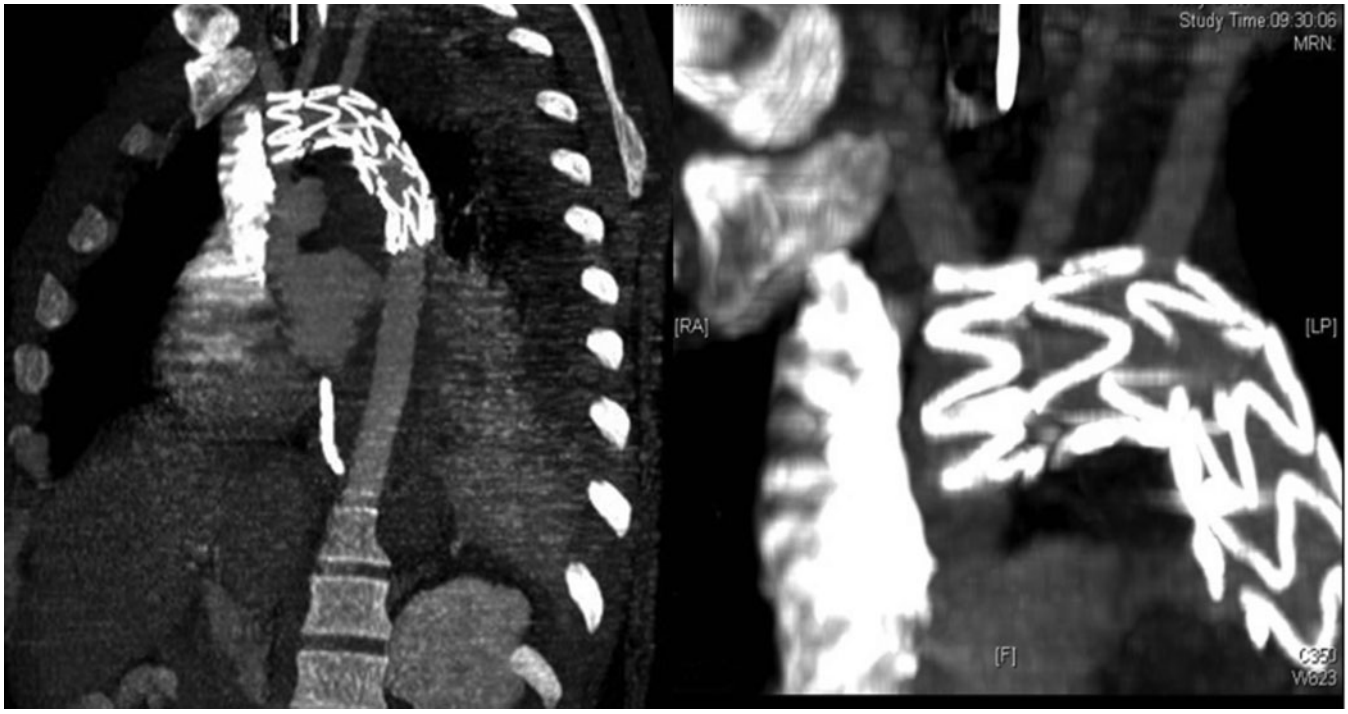

Figure 18. Traumatic aortic rupture stented CT. CT angiogram 72 h after endograft placement. This demonstrates successful repair of the ruptured aorta (left figure). There is continued forward flow in the left common carotid artery (confirmed on Doppler imaging) due to the portion of the endograft at the origin of this vessel being uncovered. The covered left subclavian artery is filling retrogradely (right figure—magnified view).

complications include stent fracture, recurrent pathology at the limit of the endograft or endoleaks.

Conclusion

Aortic pathology carries significant morbidity and mortality and requires prompt and accurate evaluation. Imaging, especially CTA and MRI, effectively diagnoses thoracic aortic disease, and is ideal for follow-up of treatment. Endovascular treatments are now a well-established alternative to conventional surgery and with advances in technology are likely to become more important.

References

1. von Kodolitsch Y, Nienaber CA, Dieckmann C, Schwartz AG, Hofmann T, Brekenfeld C, et al. Chest radiography for the diagnosis of acute aortic syndrome. Am J Med 2004;116:73–7.
2. Mirvis SE, Bidwell JK, Buddemeyer EU, Diaconis JN, Pais SO, Whitley JE, et al. Value of chest radiography in excluding traumatic aortic rupture. Radiology 1987;163:487–93.
3. Shiga T, Wajima Z, Apfel CC, Inoue T, Ohe Y. Diagnostic accuracy of transesophageal echocardiography, helical computed tomography, and magnetic resonance imaging for suspected thoracic aortic dissection: systematic review and meta-analysis. Arch Intern Med 2006;166:1350–6.
4. Brenner DJ, Hall EJ. Computed tomography—an increasing source of radiation exposure (Review). N Engl J Med 2007;357:2277–84.
5. Feuchtner GM, Jodocy D, Klauser A, Haberfellner B, Aglan I, Spoeck A, et al. Radiation dose reduction by using 100-kV tube voltage in cardiac 64-slice computed tomography: a comparative study. Eur J Radiol 2010;75:e51–6.
6. Ellis JH, Cohan RH. Reducing the risk of contrast-induced nephropathy: a perspective on the controversies. AJR Am J Roentgenol 2009;192:1544–9.
7. Ko SF, Hsieh MJ, Chen MC, Ng SH, Fang FM, Huang CC, et al. Effects of heart rate on motion artifacts of the aorta on non-ECG-assisted 0.5-sec thoracic MDCT. AJR Am J Roentgenol 2005;184:1225–30.
8. Roos JE, Willmann JK, Weishaupt D, Lachat M, Marincek B, Hilfiker PR. Thoracic aorta: motion artifact reduction with retrospective and prospective electrocardiography-assisted multi-detector row CT. Radiology 2002;222:271–7.
9. Miyazaki M, Lee VS. Nonenhanced MR angiography. Radiology 2008;248:20–43.
10. Lohan DG, Krishnam M, Tomasian A, Saleh R, Finn JP. Time-resolved MR angiography of the thorax (Review). Magn Reson Imaging Clin N Am 2008;16:235–48,viii.
11. Wolak A, Gransar H, Thomson LE, Friedman JD, Hachamovitch R, Gutstein A, et al. Aortic size assessment by noncontrast cardiac computed tomography: normal limits by age, gender, and body surface area. JACC Cardiovasc Imaging 2008;1:200–9.
12. Maldonado JA, Henry T, Gutiérrez FR. Congenital thoracic vascular anomalies (Review). Radiol Clin North Am 2010;48:85–115.
13. Hiratzka LF, Bakris GL, Beckman JA, Bersin RM, Carr VF, Casey DE Jr, et al. American College of Cardiology Foundation/American Heart Association Task Force on Practice Guidelines; American Association for Thoracic Surgery; American College of Radiology; American Stroke Association; Society of Cardiovascular Anesthesiologists; Society for Cardiovascular Angiography and Interventions; Society of Interventional Radiology; Society of Thoracic Surgeons; Society for Vascular Medicine. 2010 ACCF/AHA/AATS/ACR/ASA/SCA/SCAI/SIR/STS/SVM guidelines for the diagnosis and management of patients with Thoracic Aortic Disease: a report of the American College of Cardiology Foundation/American Heart Association

Task Force on Practice Guidelines, American Association for Thoracic Surgery, American College of Radiology, American Stroke Association, Society of Cardiovascular Anesthesiologists, Society for Cardiovascular Angiography and Interventions, Society of Interventional Radiology, Society of Thoracic Surgeons, and Society for Vascular Medicine. Circulation 2010;121:e266–369.
14. Davies RR, Gallo A, Coady MA, Tellides G, Botta DM, Burke B, et al. Novel measurement of relative aortic size predicts rupture of thoracic aortic aneurysms. Ann Thorac Surg 2006;81:169–77.
15. Elefteriades JA. Natural history of thoracic aortic aneurysms: indications for surgery, and surgical versus nonsurgical risks. Ann Thorac Surg 2002;74:S1877–80.
16. Masuda Y, Takanashi K, Takasu J, Morooka N, Inagaki Y. Expansion rate of thoracic aortic aneurysms and influencing factors. Chest 1992;102:461–6.
17. Roman MJ, Rosen SE, Kramer-Fox R, Devereux RB. Prognostic significance of the pattern of aortic root dilation in the Marfan syndrome. J Am Coll Cardiol 1993;22: 1470–6.
18. Shimada I, Rooney SJ, Farneti PA, Riley P, Guest P, Davies P, et al. Reproducibility of thoracic aortic diameter measurement using computed tomographic scans. Eur J Cardiothorac Surg 1999;16:59–62.
19. Bradshaw KA, Pagano D, Bonser RS, McCafferty I, Guest PJ. Multiplanar reformatting and three-dimensional reconstruction: for pre-operative assessment of the thoracic aorta by computed tomography. Clin Radiol 1998;53:198–202.
20. Krinsky GA, Rofsky NM, DeCorato DR, Weinreb JC, Earls JP, Flyer MA, et al. Thoracic aorta: comparison of gadolinium-enhanced three-dimensional MR angiography with conventional MR imaging. Radiology 1997;202: 183–93.
21. Krishnam MS, Tomasian A, Malik S, Desphande V, Laub G, Ruehm SG. Image quality and diagnostic accuracy of unenhanced SSFP MR angiography compared with conventional contrast-enhanced MR angiography for the assessment of thoracic aortic diseases. Eur Radiol 2010;20: 1311–20.
22. Hagan PG, Nienaber CA, Isselbacher EM, Bruckman D, Karavite DJ, Russman PL, et al. The International Registry of Acute Aortic Dissection (IRAD): new insights into an old disease. JAMA 2000;283:897–903.
23. Slater EE, DeSanctis RW. The clinical recognition of dissecting aortic aneurysm. Am J Med 1976;60:625–33.
24. Wilson SK, Hutchins GM. Aortic dissecting aneurysms: causative factors in 204 subjects. Arch Pathol Lab Med 1982;106:175–80.
25. Tsai TT, Evangelista A, Nienaber CA, Trimarchi S, Sechtem U, Fattori R, et al. International Registry of Acute Aortic Dissection (IRAD). Long-term survival in patients presenting with type A acute aortic dissection: insights from the International Registry of Acute Aortic Dissection (IRAD). Circulation 2006;114(1 Suppl):I350–6.
26. Sueyoshi E, Sakamoto I, Hayashi K, Yamaguchi T, Imada T. Growth rate of aortic diameter in patients with type B aortic dissection during the chronic phase. Circulation 2004;110(11 Suppl 1):II256–61.
27. LePage MA, Quint LE, Sonnad SS, Deeb GM, Williams DM. Aortic dissection: CTA features that distinguish true lumen from false lumen. AJR Am J Roentgenol 2001;177:207–11.
28. Williams DM, Lee DY, Hamilton BH, Marx MV, Narasimham DL, Kazanjian SN, et al. The dissected aorta: part III. Anatomy and radiologic diagnosis of branch-vessel compromise. Radiology 1997;203:37–44.
29. Morgan-Hughes GJ, Marshall AJ, Roobottom CA. Refined computed tomography of the thoracic aorta: the impact of electrocardiographic assistance. Clin Radiol 2003;58:581–8.
30. Stanson AW, Kazmier FJ, Hollier LH, Edwards WD, Pairolero PC, Sheedy PF, et al. Penetrating atherosclerotic ulcers of the thoracic aorta: natural history and clinicopathologic correlations. Ann Vasc Surg 1986;1:15–23.
31. Hayashi H, Matsuoka Y, Sakamoto I, Sueyoshi E, Okimoto T, Hayashi K, et al. Penetrating atherosclerotic ulcer of the aorta: imaging features and disease concept. Radiographics 2000;20:995–1005.
32. Kazerooni EA, Bree RL, Williams DM. Penetrating atherosclerotic ulcers of the descending thoracic aorta: evaluation with CTA and distinction from aortic dissection. Radiology 1992;183:759–65.
33. Yucel EK, Steinberg FL, Egglin TK, Geller SC, Waltman AC, Athanasoulis CA. Penetrating aortic ulcers: diagnosis with MR imaging. Radiology 1990;177:779–81.
34. Krukenberg E. Beitrage zur Frage des Aneurysma Dissecans. Beitr Pathol Anat Allg Pathol 1920;67:329–51.
35. Nienaber CA, Sievers HH. Intramural hematoma in acute aortic syndrome: more than one variant of dissection? Circulation 2002;106:284–5.
36. Evangelista A, Mukherjee D, Mehta RH, O'Gara PT, Fattori R, Cooper JV, et al. International Registry of Aortic Dissection (IRAD) Investigators. Acute intramural hematoma of the aorta: a mystery in evolution. Circulation 2005;111:1063–70.
37. Evangelista A, Mukherjee D, Mehta RH, O'Gara PT, Fattori R, Cooper JV, et al. International Registry of Aortic Dissection (IRAD) Investigators. Acute intramural hematoma of the aorta: a mystery in evolution. Circulation 2005;111:1063–70.
38. Bosma MS, Quint LE, Williams DM, Patel HJ, Jiang Q, Myles JD. Ulcerlike projections developing in noncommunicating aortic dissections: CT findings and natural history. AJR Am J Roentgenol 2009;193:895–905.
39. Sueyoshi E, Matsuoka Y, Imada T, Okimoto T, Sakamoto I, Hayashi K. New development of an ulcerlike projection in aortic intramural hematoma: CT evaluation. Radiology 2002;224:536–41.
40. Murray JG, Manisali M, Flamm SD, VanDyke CW, Lieber ML, Lytle BW, et al. Intramural hematoma of the thoracic aorta: MR image findings and their prognostic implications. Radiology 1997;204:349–55.
41. Richens D, Kotidis K, Neale M, Oakley C, Fails A. Rupture of the aorta following road traffic accidents in the United Kingdom 1992–1999. The results of the co-operative crash injury study. Eur J Cardiothorac Surg 2003;23:143–8.
42. Richens D, Field M, Neale M, Oakley C. The mechanism of injury in blunt traumatic rupture of the aorta. Eur J Cardiothorac Surg 2002;21:288–93.
43. Crass JR, Cohen AM, Motta AO, Tomashefski JF Jr, Wiesen EJ. A proposed new mechanism of traumatic aortic rupture: the osseous pinch. Radiology 1990;176:645–9.
44. Cohen AM, Crass JR, Thomas HA, Fisher RG, Jacobs DG. CT evidence for the ''osseous pinch'' mechanism of traumatic aortic injury. AJR Am J Roentgenol 1992;159:271–4.
45. Steenburg SD, Ravenel JG. Acute traumatic thoracic aortic injuries: experience with 64-MDCT. AJR Am J Roentgenol 2008;191:1564–9.
46. Sammer M, Wang E, Blackmore CC, Burdick TR, Hollingworth W. Indeterminate CT angiography in blunt thoracic trauma: is CT angiography enough? AJR Am J Roentgenol 2007;189:603–8.
47. Gatzoulis M, Swan L, Therrien J, Pantely G, editors. Adult congenital heart disease: a practical guide. Oxford: Blackwell Publishing; 2005.
48. Crafoord C, Nylan G. Congenital coarctation of the aorta and its surgical treatment. J Thorac Surg 1945;14:347–61.
49. Jenkins NP, Ward C. Coarctation of the aorta: natural history and outcome after surgical treatment. QJM 1999;92:365–71.

50. Puranik R, Tsang VT, Puranik S, Jones R, Cullen S, Bonhoeffer P, et al. Late magnetic resonance surveillance of repaired coarctation of the aorta. Eur J Cardiothorac Surg 2009;36:91–5.
51. Kaushal S, Backer CL, Patel JN, Patel SK, Walker BL, Weigel TJ, et al. Coarctation of the aorta: midterm outcomes of resection with extended end-to-end anastomosis. Ann Thorac Surg 2009;88:1932–8.
52. Pandey R, Jackson M, Ajab S, Gladman G, Pozzi M. Subclavian flap repair: review of 399 patients at median follow-up of fourteen years. Ann Thorac Surg 2006;81:1420–8.
53. Walhout RJ, Lekkerkerker JC, Oron GH, Hitchcock FJ, Meijboom EJ, Bennink GB. Comparison of polytetrafluoroethylene patch aortoplasty and end-to-end anastomosis for coarctation of the aorta. J Thorac Cardiovasc Surg 2003;126:521–8.
54. Warnes CA, Williams RG, Bashore TM, Child JS, Connolly HM, Dearani JA, et al. ACC/AHA 2008 Guidelines for the Management of Adults with Congenital Heart Disease: a report of the American College of Cardiology/American Heart Association Task Force on Practice Guidelines (writing committee to develop guidelines on the management of adults with congenital heart disease). Circulation 2008;118:e714–833.
55. Thanopoulos BV, Eleftherakis N, Tzanos K, Skoularigis I, Triposkiadis F. Stent implantation for adult aortic coarctation. J Am Coll Cardiol 2008;52:1815–16.
56. Holzer R, Qureshi S, Ghasemi A, Vincent J, Sievert H, Gruenstein D, et al. Stenting of aortic coarctation: acute, intermediate, and long-term results of a prospective multi-institutional registry—Congenital Cardiovascular Interventional Study Consortium (CCISC). Catheter Cardiovasc Interv 2010;76:553–63.
57. Didier D, Saint-Martin C, Lapierre C, Trindade PT, Lahlaidi N, Vallee JP, et al. Coarctation of the aorta: pre and postoperative evaluation with MRI and MR angiography; correlation with echocardiography and surgery. Int J Cardiovasc Imaging 2006;22:457–75.
58. Therrien J, Thorne SA, Wright A, Kilner PJ, Somerville J. Repaired coarctation: a ''cost-effective'' approach to identify complications in adults. J Am Coll Cardiol 2000; 35:997–1002.
59. Ming Z, Yumin Z, Yuhua L, Biao J, Aimin S, Qian W. Diagnosis of congenital obstructive aortic arch anomalies in Chinese children by contrast-enhanced magnetic resonance angiography. J Cardiovasc Magn Reson 2006;8:747–53.
60. Hom JJ, Ordovas K, Reddy GP. Velocity-encoded cine MR imaging in aortic coarctation: functional assessment of hemodynamic events. Radiographics 2008;28:407–16.
61. Steffens JC, Bourne MW, Sakuma H, O'Sullivan M, Higgins CB. Quantification of collateral blood flow in coarctation of the aorta by velocity encoded cine magnetic resonance imaging. Circulation 1994;90:937–43.
62. Kenny D, Hamilton MC, Martin RP. Stainless steel stents and magnetic resonance imaging looking into a black hole. J Am Coll Cardiol 2009;54:2202–3.
63. Pujadas S, Reddy GP, Weber O, Tan C, Moore P, Higgins CB. Phase contrast MR imaging to measure changes in collateral blood flow after stenting of recurrent aortic coarctation: initial experience. J Magn Reson Imaging 2006;24:72–6.
64. Sridharan S, Yates R, Taylor AM. Optimizing imaging after coarctation stenting: the clinical utility of multidetector computer tomography. Catheter Cardiovasc Interv 2005;66: 420–3.
65. Collins N, Mahadevan V, Horlick E. Aortic rupture following a covered stent for coarctation: delayed recognition. Catheter Cardiovasc Interv 2006;68:653–5.
66. Arend WP, Michel BA, Bloch DA, Hunder GG, Calabrese LH, Edworthy SM, et al. The American College of Rheumatology 1990 criteria for the classification of Takayasu arteritis. Arthritis Rheum 1990;33:1129–34.
67. Sharma BK, Jain S, Suri S, Numano F. Diagnostic criteria for Takayasu arteritis. Int J Cardiol 1996;54(Suppl.):S141–7.
68. Park JH, Chung JW, Im JG, Kim SK, Park YB, Han MC. Takayasu arteritis: evaluation of mural changes in the aorta and pulmonary artery with CT angiography. Radiology 1995;196:89–93.
69. Gotway MB, Araoz PA, Macedo TA, Stanson AW, Higgins CB, Ring EJ, et al. Imaging findings in Takayasu's arteritis. AJR Am J Roentgenol 2005;184:1945–50.
70. Steeds RP, Mohiaddin R. Takayasu arteritis: role of cardiovascular magnetic imaging. Int J Cardiol 2006;109:1–6.
71. Choe YH, Kim DK, Koh EM, Do YS, Lee WR. Takayasu arteritis: diagnosis with MR imaging and MR angiography in acute and chronic active stages. J Magn Reson Imaging 1999;10:751–7.
72. Tso E, Flamm SD, White RD, Schvartzman PR, Mascha E, Hoffman GS. Takayasu arteritis: utility and limitations of magnetic resonance imaging in diagnosis and treatment. Arthritis Rheum 2002;46:1634–42.
73. Nuenninghoff DM, Hunder GG, Christianson TJ, McClelland RL, Matteson EL. Incidence and predictors of large-artery complication (aortic aneurysm, aortic dissection, and/or large-arterystenosis) in patients with giant cell arteritis: a population-based study over 50 years. Arthritis Rheum 2003;48:3522–31.
74. Zidi A, Ben Miled Mrad K, Hantous S, Nouira K, Mestiri I, Mrad S. [Thoracic involvement in Behcet's vasculitis]. J Radiol 2006;87:285–9.
75. Lopes RJ, Almeida J, Dias PJ, Pinho P, Maciel MJ. Infectious thoracic aortitis: a literature review. Clin Cardiol 2009;32:488–90.
76. Lee WK, Mossop PJ, Little AF, Fitt GJ, Vrazas JI, Hoang JK, et al. Infected (mycotic) aneurysms: spectrum of imaging appearances and management. Radiographics 2008;28:1853–68.
77. Lee MH, Chan P, Chiou HJ, Cheung WK. Diagnostic imaging of Salmonella-related mycotic aneurysm of aorta by CT. Clin Imaging 1996;20:26–30.
78. Lin MP, Chang SC, Wu RH, Chou CK, Tzeng WS. A comparison of computed tomography, magnetic resonance imaging, and digital subtraction angiography findings in the diagnosis of infected aortic aneurysm. J Comput Assist Tomogr 2008;32:616–20.
79. Macedo TA, Stanson AW, Oderich GS, Johnson CM, Panneton JM, Tie ML. Infected aortic aneurysms: imaging findings. Radiology 2004;231:250–7. Erratum in: Radiology 2006;238:1078.
80. Hoang JK, Martinez S, Hurwitz LM. MDCT angiography after open thoracic aortic surgery: pearls and pitfalls. AJR Am J Roentgenol 2009;192:W20–7.
81. Quint LE, Francis IR, Williams DM, Monaghan HM, Deeb GM. Synthetic interposition grafts of the thoracic aorta: postoperative appearance on serial CT studies. Radiology 1999;211:317–24.
82. Dake MD, Miller DC, Semba CP, Mitchell RS, Walker PJ, Liddell RP. Transluminal placement of endovascular stent grafts for the treatment of descending thoracic aortic aneurysms. N Engl J Med 1994;331:1729–34.
83. Leurs LJ, Bell R, Degrieck Y, Thomas S, Hobo R, Lundbom J, et al. Endovascular treatment of thoracic aortic diseases: combined experience from the EUROSTAR and United Kingdom thoracic endograft registries. J Vasc Surg 2004;40:670–9.
84. Brown K, Eskandari MK, Matsumura JS, Rodriguez H, Morasch MD. Short and mid-term results with minimally invasive endovascular repair of acute and chronic thoracic aortic pathology. J Vasc Surg 2008;47:714–23.
85. Bavaria JE, Appoo JJ, Makaroun MS, Verter J, Yu ZF, Mitchell RS. Endovascular stent grafting versus open surgical repair of descending thoracic aortic aneurysms in low-risk patients: a multi-center comparative trial. J Thorac Cardiovasc Surg 2007;133:369–77.

86. Fattori R, Nienaber CA, Rousseau H, Beregi JP, Heijmen R, Grabenwöger M, et al. Results of endovascular repair of the thoracic aorta with the Talent thoracic stent graft: the Talent thoracic retrospective registry. J Thorac Cardiovasc Surg 2006;132:332–9.
87. Rousseau H, Dambrin C, Marcheix B, Richeux L, Mazerolles M, Cron C, et al. Acute traumatic aortic rupture: a comparison of surgical and stent-graft repair. J Thorac Cardiovasc Surg 2005;129:1050–5.
88. Coselli JS, Bozinovski J, LeMaire SA. Open surgical repair of 2286 thoracoabdominal aortic aneurysms. Ann Thorac Surg 2007;83:S862–4.
89. Conrad MF, Crawford RS, Davison JK, Cambria RP. Thoracoabdominal aneurysm repair: a 20 year perspective. Ann Thorac Surg 2007;83:856–61.
90. Buth J, Harris PL, Hobo R, van Eps R, Cuypers P, Duijm L, et al. Neurologic complications associated with endovascular repair of thoracic aortic pathology: Incidence and risk factors. a study from the Europern Collaborators on Stent/Graft Techniques for Aortic Aneurysm Repair (EUROSTAR) registry. J Vasc Surg 2007;46:1103–10.
91. Feezor RJ, Martin TD, Hess PJ Jr, Daniels MJ, Beaver TM, Klodell CT, et al. Extent of aortic coverage and incidence of spinal cord ischaemia after endovascular thoracic aneurysm repair. Ann Thorac Surg 2008;86:1809–14.
92. Nakayama Y, Awai K, Yanaga Y, Nakaura T, Funama Y, Hirai T, et al. Optimal contrast medium injection protocols for the depiction of the Adamkiewicz artery using 64-detector CT angiography 2008;63:880–7.
93. Kotelis D, Geisbüsch P, Hinz U, Hyhlik-Dürr A, von Tengg-Kobligk H, Allenberg JR, et al. Short and mid term results after left subclavian artery coverage during endovascular repair of thoracic aorta. J Vasc Surg 2009;50: 1285–92.